Civil Engineering and Architecture 13(6): 4165-4178, 2025 http://www.hrpub.org
DOI: 10.13189/cea.2025.130606

PID Controlled Semi-Active Device for FPS Isolated Structure

B. Durga Prasad Baliga[1], Jagadeesha Pai B.[1,*], I. Thirunavukkarasu[2]

[1]Department of Civil Engineering, Manipal Institute of Technology, Manipal Academy of Higher Education, Manipal - 576104, Karnataka, India
[2]Department of Instrumentation & Control Engineering, Manipal Institute of Technology, Manipal Academy of Higher Education, Manipal - 576104, Karnataka, India

Received May 5, 2025; Revised September 12, 2025; Accepted October 14, 2025

Cite This Paper in the Following Citation Styles

***(a):** [1] B. Durga Prasad Baliga, Jagadeesha Pai B., I. Thirunavukkarasu , "PID Controlled Semi-Active Device for FPS Isolated Structure," Civil Engineering and Architecture, Vol. 13, No. 6, pp. 4165 - 4178, 2025. DOI: 10.13189/cea.2025.130606.*

***(b):** B. Durga Prasad Baliga, Jagadeesha Pai B., I. Thirunavukkarasu (2025). PID Controlled Semi-Active Device for FPS Isolated Structure. Civil Engineering and Architecture, 13(6), 4165 - 4178. DOI: 10.13189/cea.2025.130606.*

Abstract The friction pendulum system (FPS) is a popular base isolation device to minimize seismic forces transferred to the structures. Constant isolator frequency of FPS may produce the resonance problem in the isolated structure for near-fault earthquake ground motions. So FPS may have limited effectiveness in isolating structures subjected to certain types of seismic activity. For improving the performance of such structures, a control system may be very useful to obtain the desired results. To address this issue, a PID controlled semi-active device is proposed in this study. PID algorithm is widely used in the industries and compared to other controllers, PID is simple and has a clear physical meaning. The structural model and the isolator properties considered for the isolated structure are developed as state-space matrices and are converted into transfer functions. Using BODE approximations, second-order plus dead time (SOPDT) models for these higher order transfer functions are derived to attain PID parameters. The PID parameters are tuned by means of Routh- Hurwitz technique. The usefulness of the proposed technique is established through numerical simulations for FPS isolated structures with two degrees of freedom. Results of the investigations indicate that a PID controller reduces shear at the base and sliding displacement of the structure isolated with FPS simultaneously. Furthermore, the resonance problem of FPS isolated structure can be nullified using the proposed technique.

Keywords PID Controller, Semi-Active Device, Base Isolation, Friction Pendulum System, Earthquake Ground Motion

1. Introduction

Base isolation is a popular passive structural control method for minimizing force transfer to structures. It essentially isolates the structure and its contents from hazardous ground motions, particularly in the frequency range where the building is most vulnerable [1]. Among the numerous base isolation systems, the Friction Pendulum System (FPS) suggested by Zayas et al. [2] is highly popular. FPS utilizes pendulum-like motion to lengthen the natural period of the decoupled structure, effectively bypassing the most intense earthquake forces [3]. FPS integrates sliding and re-centering mechanisms into one unit, featuring a spherical shaped sliding surface [4]. Restoring force in this system is because of the curved sliding surface of FPS, and hence the isolation period depends only on the radius of sliding surface and is free from superstructure mass. However, the spherical sliding surface of FPS introduces a constant isolation frequency to the decoupled structure [5]. Hence, structure response varies with the type of seismic event, and the isolation may not be effective for near-fault (NF) earthquakes, which typically have a frequency near the frequency of isolator.

Many control techniques such as passive, active and semi-active are proposed over time for improving the performance of isolated structure. Passive control devices, enhance damping or the stiffness of the isolation system adopting rubber bearings of high damping, friction dampers, metallic yield dampers, viscous fluid dampers, tuned mass dampers, etc. The foremost benefit of such devices is they operate without the requirement of an external source. However, reduced efficiency at low frequencies, lack of robustness, and the system's larger size and weight limit its efficiency and usage in the structural control [6]. The active systems, on the other hand, consist of control devices which change their properties in real-time. The structural system with an active control strategy can be provided with computer-controllable forces [7]. Extensive investigations on these systems have indicated that active systems perform well for a wide range of earthquakes and have number of advantages when compared to passive control techniques [6], [8-17]. Few benefits include greater efficacy in response control, less sensitivity to site-specific situations and ground movement, viability in multiple hazard reduction circumstances and specificity of control objectives [18]. However, a significant limitation of active systems is their large power requirement. Semi-active devices offer a low-power solution to enhance active system applicability. This approach combines the reliability of a passive control scheme with the flexibility of an active control scheme [19]. These devices control structural response without injecting mechanical energy, ensuring efficient property adjustment for reduced system response while guaranteeing bounded input-output stability. The effectiveness of semi-active control techniques was investigated by many researchers [18], [20-44]. Semi-active devices perform like active devices without large power requirements making them reliable during earthquakes [44]. The distinction between semi-active and active control remains unclear owing to the scarcity of a strong definition of the extent of energy [7]. To attain optimum structural performance, parameters of active or semi-active devices are tuned using control algorithm. Hence, the usefulness of a control system is primarily governed by robustness of control stratagy adopted to tune the device. Some of the popular control algorithms recommended for structural control are H-infinity, fuzzy logic, neural network and PID. Among these, the PID control has widespread adoption in industries and compared to other controllers, PID is simple and physically meaningful [45]. This approach is highly effective and applicable to a broad range of problems [46]. Application of a PID controller to regulate the actuator force has been investigated [47, 48] in the vibration analysis of beams. There exist few applications of PID controller to control the response of structures subjected to earthquakes. Guclu [12] compared the vibration of a MDOF structure under Marmara earthquake (Turkey 1999) using PID and SMC controllers and found the SMC controller giving better results than the simple PID controller. Guclu and Yazici [49] studied the response of a MDOF structure fixed at the base using PID and FLC controller for an active seismic device and demonstrated the efficacy of FLC controller. Guclu and Yazici [50] also proposed a Fuzzy PID type controller (including PI and PID) to increase the seismic control capability for the fixed base MDOF structure with active tuned dampers resulting in superior vibration control. Etedali et al. [51] proposed an optimal PID controller having piezoelectric friction dampers (PFD) to control structure response isolated at the base with linear rubber bearing. PID controller tuned using a genetic algorithm was used to regulate the performance of PFD in the study. Nigdeli and Boduroglu [52] proposed active tendon control systems tuned with PID controllers for torsionally irregular structures. Etedali and Tavakoli [53] presented a multi-objective optimization approach for designing PD and PID controllers to mitigate seismic effects in high-rise buildings. Sen et al. [54] utilized Bees algorithm to optimize PID controller gains for effective active vibration control in structures. Heidari et al. [55] proposed a control strategy integrating PID and LQR algorithms for earthquake response reduction in structures equipped with active tuned mass dampers (ATMD). Wang et al. [56] evaluated PID, LQR, and fuzzy controller performance in semi-active base isolation systems using magnetorheological dampers under uncertain seismic inputs using numerical simulations, and concluded they were effective only for specific seismic motions they were optimized for, highlighting their limited adaptability to varying seismic conditions. Bhowmik et al. [57] studied the performance of a MDOF isolated structure using magnetorheological dampers adopting LQG and PID controller and concluded that LQG-technique is effective in reducing responses than PID for MDOF isolated structures. Sharma et al. [58] studied MR damper's efficiency to control damping force by applying magnetic field externally. Investigations of Vides et al. [59] on base isolated structures having viscous fluid dampers reveal a considerable reduction in responses against fixed structures and also suggest adopting advanced control techniques like PID and H-infinity to obtain better results. From the literatures, it is seen that the PID controller has distinct physical importance and therefore is widely used for 2DOF structures with fixed base in controlling structural response. Although, there is well developed research work on PID for the fixed base structure, its application to control the structure isolated with FPS remains limited. In this paper, a PID controlled semi-active device is presented to study the base shear, isolating displacement and control force to enhance performance in structures isolated with FPS.

2. Analytical Modeling of Structure Isolated with FPS

Figure 1 displays a two degrees-of-freedom (2DOF) FPS isolated structure. As seen in figure an additional control force is applied at the base through a semi-active PID controlled device. A semi-active variable orifice fluid damper (VFD) is externally attached between the foundation and basement of the superstructure, providing supplemental damping to the isolation system. Wongprasert et al. [24] have also proposed a similar device to control the MDOF structure isolated with FPS bearing. The damper device can be modeled as a linear viscous dashpot for earthquake safety solutions [23, 24].

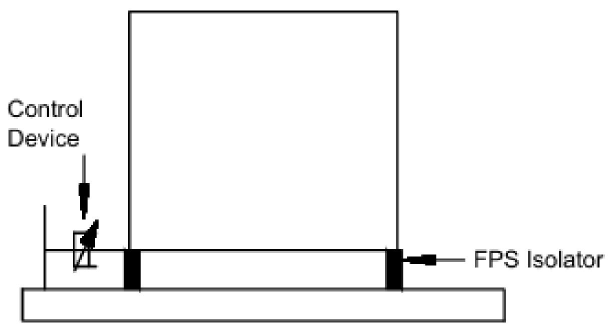

Figure 1. A 2DOF isolated structure with a control device

The isolator force F_r of FPS isolator is expressed in equation 1 [4].

$$F_r = k_b \ \ x_b \tag{1}$$

where, $k_b = m \ \frac{g}{R}$, m: mass on each isolator, g: is gravitational acceleration, R: radius of FPS isolator, and x_b: sliding displacement. A structure resting on FPS isolators undergoes cyclic phases of sliding and non-sliding phases. The structure initially remains in a non-sliding phase until the earthquake-induced horizontal force at base exceeds the resistance of friction of the isolator. However, once base force exceeds base frictional resistance, sliding commences at base indicating in sliding phase. During the sliding phase, when base velocity reaches zero, the structure either moves back to the non-sliding phase or reverses its sliding direction. Thus, an isolated structure undergoes a sequence of alternating sliding and non-sliding phases during seismic excitation. In order to model these phases, a technique presented by Yang et al. [60] is used for proposed analysis. Similar procedure has also been used by Krishnamoorthy et al. [37] in modelling a structure isolated by FPS. In this technique, at the base a fictitious spring is attached as shown in Figure 1. For non-sliding, spring stiffness is assigned a large value, while it's set to zero when sliding occurs.

During the non-sliding phase, the equation of motion of the isolated structure is governed by

$$M \ \ \ddot{x} + C \ \ \dot{x} + K \ \ x = F(t) \tag{2}$$

and during sliding phase is

$$M \ \ \ddot{x} + C \ \ \dot{x} + K \ \ x = F(t) + F_b \tag{3}$$

where, M: mass matrix, C: damping matrix, K: stiffness matrix of the structure respectively. $\ddot{x}$: acceleration, $\dot{x}$: velocity, x: displacement vectors relative with ground respectively. Vector of disturbance force $F(t)$, caused by ground acceleration $\ddot{x}_g(t)$, is

$$F(t) = -M \ \ \ddot{x}_g(t) \tag{4}$$

F_b is force acting at the base consisting of (i) maximum frictional resistance F_s (ii) restoring force of isolator F_r and (iii) actuator control force F_c. Thus, F_b can be expressed as

$$F_b = -F_s \ \ sgn(\dot{x}_b) - F_r - F_c \tag{5}$$

$\dot{x}_b$: relative base velocity and sgn: signum function. Notably, isolator forces F_s and F_r are purely passive and uncontrollable, whereas F_c is a controllable force and makes this analysis different from the conventional analysis of FPS isolated structure.

2.1. PID Controller

The PID control strategy integrates proportional control, integral control, and derivative control. The collective control action, F_c determined by the PID controller is

$$F_c = k_p \ \ \mathrm{e}(t) + k_d \frac{de(t)}{dt} + k_i \int e(t) \ \ dt \tag{6}$$

where, k_p: proportional gain, k_d: derivative gain, k_i: integral gain, and $e(t)$: error terms represent discrepancy in desired and measured responses. The PID controller reduces the error by regulating inputs of process control. From equation 6, it can be observed that three parameters k_p, k_d and k_i are to be determined to tune PID controller. In the proposed study, a technique suggested by Wang et al. [61] is adopted to tune parameters of PID. Thirunavukkarasu et al. [62] have also used a similar technique to tune the PID parameters in the study of a distillation column for the chemical and processing industries. In this technique, PID parameters are tuned using Bode plot and Routh-Hurwitz method [63]. A simplified, reduced-order model is proposed to capture the dominant dynamic characteristics, ensuring high and consistent performance across processes with diverse dynamics. A second-order plus dead time (SOPDT) model, as in equation 7, is obtained from Bode approximation of a higher order transfer function.

$$G(s) = \frac{e^{-st_0}}{as^2+bs+c} \tag{7}$$

Using the iterative method, the numerical inputs 'a', $'b'$ and $'c'$ of SOPDT model are varied so that the plot of transfer functions matches with the standard BODE Plot. The objective of reducing the higher order transfer function using BODE approximations is to enhance the response of system in determining PID parameters. Solving the normalized model as proposed by Wang et al. [61], a quadratic equation in terms of delayed function t_0 can be computed. The Routh-Hurwitz criterion is applied to determine stability bounds for tuning the controller. In the proposed study, the required control force, F_c is regulated by adopting a variable orifice fluid damper.

The present study proposes utilizing a variable orifice fluid damper (VFD) to regulate necessary control force F_c. The output force of damper F_d having damping coefficient C_d is expressed as

$$F_d = C_d \; \dot{x}_b \tag{8}$$

For the proposed control system, as proposed by Wongprasert and Symans [24], the damping coefficient C_d is varied to minimize the difference between damper force F_d (given by equation 8) and the desired control force F_c. Thus, the controlled coefficient of damping C_d is given by

$$C_d = F_c \;/\; \dot{x}_b \tag{9}$$

3. Numerical Application

The proposed PID control scheme to control the semi-active device for FPS isolated structure is demonstrated numerically for 2DOF structural model shown in Figure 1. Structural matrices and isolator properties used for simulation of the isolated structure model are analogous to those used by Lu et al. [28]. In addition to the isolator force, an appropriate level of control force also acts at the base as shown in Figure 1.

Besides the isolator force, a suitable control force is also applied at the base.

$$M = \begin{bmatrix} 100 & 0 \\ 0 & 300 \end{bmatrix} \; kNs^2/m$$

$$C = \begin{bmatrix} 314.1 & -314.1 \\ -314.1 & 314.1 \end{bmatrix} kNs/m$$

$$K = \begin{bmatrix} 32890 & -32890 \\ -32890 & 32890 \end{bmatrix} kN/m$$

radius of FPS, R = 1.55 m and sliding surface frictional coefficient, $\mu =$ 0.03.

The stiffness matrices of the isolation system and combined structure-isolation system are

$$K_I = \begin{bmatrix} 2527 & 0 \\ 0 & 0 \end{bmatrix} kN/m$$

$$K = \begin{bmatrix} 35417 & -32890 \\ -32890 & 32890 \end{bmatrix} kN/m$$

The state space matrices A, B, C, and D for structure are

$$A = \begin{bmatrix} 0 & I \\ -\frac{K}{M} & -\frac{C}{M} \end{bmatrix} =$$

$$\begin{bmatrix} 0 & 0 & 1 & 0 \\ 0 & 0 & 0 & 1 \\ -354.17 & 328.9 & -3.141 & 3.141 \\ 109.63 & -109.63 & 1.047 & -1.047 \end{bmatrix}$$

For Control Force provided at the base

$$B_0 = \begin{bmatrix} 0 \\ 0 \\ 1 \\ 1 \end{bmatrix}$$

$$B = \begin{bmatrix} 0 \\ 0 \\ -\frac{B_0}{M_1} \\ -\frac{B_0}{M_2} \end{bmatrix} = \begin{bmatrix} 0 \\ 0 \\ -\frac{1}{100} \\ -\frac{1}{300} \end{bmatrix}$$

$$C = \begin{bmatrix} 1 & 0 & 0 & 0 \\ 0 & 1 & 0 & 0 \end{bmatrix}; \quad D = \begin{bmatrix} 0 \\ 0 \end{bmatrix}$$

The Transfer Functions for the above state space matrices $A, B, C,$ and D are

$$[\mathrm{C}][sI - A]^{-1}[\mathrm{B}] = \frac{3.21 \; s^2 - 0.35 \; s - 27.7}{s^4 + 4.2 \; s^3 + 463.8 \; s^2 + 26.46 \; s + 2770.35} \tag{10}$$

and

$$\frac{-2.96 \; s^2 - 0.0016 \; s - 8.31}{s^4 + 4.2 \; s^3 + 463.8 \; s^2 + 26.46 \; s + 2770.35} \tag{11}$$

The SOPDT models as shown in equations 12 and 13 are obtained using MATLAB BODE approximation for the higher order transfer functions given by equations 10 and 11. A comparison of standard Bode graphs with Bode graphs for transfer functions is shown in Figures 2-3. Further equation 12 is considered for normalization since it matches appreciably with the standard Bode plot as shown in Figure 2.

$$\mathrm{G(s1)} = \left(\frac{100}{22 \; s^2 \; + \; 100 \; s \; + \; 10000}\right) \; e^{(-1*s)} \tag{12}$$

$$\mathrm{G(s2)} = \left(\frac{70}{25 \; s^2 + 100 \; s \; + 25000}\right) \; e^{(-1*s)} \tag{13}$$

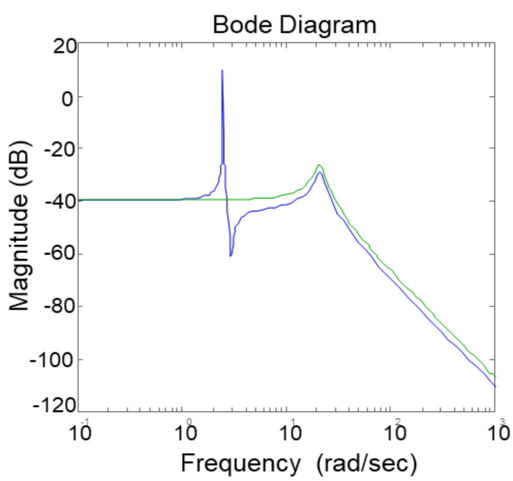

Figure 2. Approximation of the 4th order system to 2nd order continuous-time transfer function with delay for equation 12

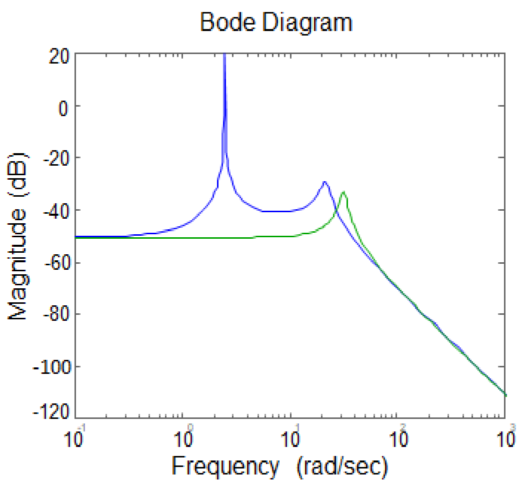

Figure 3. Approximation of the 4th order system to 2nd order continuous-time transfer function with delay for equation 13

The normalized transfer function is given in equation 12.

$$\text{G(s1NOR)} = \left(\frac{1}{0.22\ s^2 + s\ +100}\right)\ e^{(-0.01*s)} \quad (14)$$

A PID controller is represented as

$$K(s) = k_p + \frac{K_i}{s} + \ k_d s \quad (15)$$

Frequency response $G(s)H(s)$) for equation 14 is obtained by putting $s = j\omega$ (where: $j^2 = -1$) such that two different points $s = j\omega_c$ and $s = j\omega_b$ are selected to satisfy the following conditions

$$G(jw_c) = |G(jw_c)| \angle G(jw_c) \leq -\ \pi \quad (16)$$

$$G(jw_b) = |G(jw_b)| \angle G(jw_b) \angle G(jw_b) \leq \frac{-\pi}{2} \quad (17)$$

Frequency Response $G(s)H(s)$ is

$$G(s)H(s) = \left(\frac{1}{0.22\ (j\omega)^2\ +\ (j\omega)\ +100}\right)\ e^{(-0.01*j\omega)} \quad (18)$$

$$Rewriting,\ = \frac{e^{(-0.01*j\omega)}}{(100\ -\ 0.22\ \omega^2) + j\omega} \quad (19)$$

Thus,

$$\angle G(s)H(s) = -180° - 0.01\omega - \tan^{-1}\left(\frac{\omega}{100-0.22\ \omega^2}\right) \quad (20)$$

$$= -179.76° < -180°\ \text{ when } \omega = \omega_c = 162°,$$

and

$$= -90.03° \cong\ -90°\ \text{ when } \omega = \omega_b =\ 21.32°.$$

Using ω_c and ω_b, the two magnitudes are

$$|G(s)H(s)| = \frac{1}{\sqrt{(100 - 0.22\ x\ 162)^2 + 162^2}}$$

$$=1.76\ X\ 10^{-4}$$

$$|G(s)H(s)| = \frac{1}{\sqrt{(100 - 0.22\ x\ 21.32)^2 + 21.32^2}}$$

$$=\ 46.89\ X\ 10^{-3}$$

The real part and imaginary part of the normalized transfer function equation 14 are expressed as

$$c - a\omega_c^2 = \frac{\cos(\omega_c t_0)}{-|G(j\omega_c)|} \quad (21)$$

$$b\omega_c = \frac{\sin(\omega_c t_0)}{|G(j\omega_c)|} \quad (22)$$

$$c - a\omega_b^2 = \frac{\sin(\omega_b t_0)}{|G(j\omega_b)|} \quad (23)$$

$$b\omega_b = \frac{\cos(\omega_b t_0)}{|G(j\omega_b)|} \quad (24)$$

To obtain t_0 an assumption made is

$$\frac{\sin(\omega_c t_0)}{cos(\omega_b t_0)} = \frac{\omega_c |G(j\omega_c)|}{\omega_b |G(j\omega_b)|} = \Omega \quad (25)$$

$$\Omega = \frac{162\ x\ 1.76\ X\ 10^{-4}}{21.32\ x\ 46.89\ X\ 10^{-3}} = 0.0285$$

Sine and cosine functions approximated by second-order polynomials give

$$p(\omega_c^2 - \Omega\omega_b^2)L^2 + (q\omega_c + \Omega r\omega_b)L - \Omega = 0 \quad (26)$$

The constants $p, q,$ and r are

$$p = \left(\frac{8}{\pi^2}\right)(1-\sqrt{2}) = -0.34$$

$$q = \left(\frac{2}{\pi}\right)(2\sqrt{2}-1) = 1.164$$

$$r = \left(\frac{2}{\pi}\right)(2\sqrt{2}-3) = 0.11$$

Thus, equation 26 is

$$-0.34(162^2 - 0.0285x21.32^2)\ t_o^2\ \ + ((1.164x162 - 0.0285\ \ (-0.11)\ \ (21.32))\ t_0 - 0.0285\ \ = 0 \quad (27)$$

The delayed function of the quadratic equation 27 is the absolute least value obtained as $t_0 = 1.52\ \ x\ \ 10^{-4}$

The coefficients a, b, and c obtained are

$$a = \frac{1}{\omega_c^2 - \omega_b^2}\left[\frac{\sin(\omega_b t_0)}{|G(j\omega_b)|} + \frac{cos(\omega_c t_0)}{|G(j\omega_c)|}\right] \quad (28)$$

$$= \frac{1}{162^2 - 21.32^2}\left[\frac{\sin(21.32x1.52x10^{-4})}{46.89x10^{-3}} + \frac{\cos(162x1.52x10^{-4})}{1.76x10^{-4}}\right] = 0.22$$

$$b = \frac{sin(\omega_c t_0)}{\omega_c |G(j\omega_c)|} \quad (29)$$

$$= \frac{sin(162x1.52x10^{-4})}{162x1.76x10^{-4}} = 0.015$$

$$c = \frac{1}{\omega_c^2 - \omega_b^2}\left[\omega_c^2 \frac{\sin(\omega_b t_0)}{|G(j\omega_b)|} +\ \omega_b^2 \frac{cos(\omega_c t_0)}{|G(j\omega_c)|}\right] \quad (30)$$

$$= \frac{1}{162^2 - 21.32^2} 162^2 \left[\frac{\sin(21.32x1.52x10^{-4})}{46.89x10^{-3}} + 21.32^2 \frac{cos(162x1.52x10^{-4})}{1.76x10^{-4}}\right] = 100.08$$

The PID parameters are further tuned using the Routh-Huwitz technique as proposed by Wang et al. [60].

$$b^2 - 4ac = 0.015^2 - 4\ x\ 0.22\ x\ 100.08$$

$$= -88.07 < 0$$

$$\frac{1}{\tau} = \frac{b}{2a} = \frac{0.015}{2\ x\ 0.22} = 0.034$$

$$\epsilon_0 = \frac{b}{2\sqrt{ac}} = \frac{0.015}{2\sqrt{0.22x100.08}}$$

$$= 1.598\ x\ 10^{-3} \quad < \epsilon_n = 0.7071$$

$$\text{For} \quad \epsilon_n \leq 0.7071,\ k = \frac{1}{\tau} e^{-\left(\frac{t_0}{\tau}\right)} \tag{31}$$

Tuning parameter,

$$k = 0.034\ \ e^{-\left(1.52x10^{-4}\right)\ x\ 0.034} \ = 0.034$$

Tuning parameter,

$$k = 0.034\ \ e^{-\left(1.52x10^{-4}\right)\ x\ 0.034} \ = 0.034$$

The tuned PID controller parameters are

$$\begin{bmatrix} k_P \\ k_I \\ k_D \end{bmatrix} = k \begin{bmatrix} b \\ c \\ a \end{bmatrix} = 0.034 \begin{bmatrix} 0.015 \\ 100.08 \\ 0.22 \end{bmatrix} = \begin{bmatrix} 0.00051 \\ 3.40272 \\ 0.00748 \end{bmatrix}$$

A PID controller obtained is

$$K(s) = 0.00051 + \frac{3.40272}{s} + 0.00748s$$

The efficiency of the proposed controller is studied in two parts. In the first part, the usefulness of the technique is studied for sinusoidal ground acceleration with varying excitation frequency, and in the second part, the efficacy of the controller is studied for real time earthquakes. Structural responses chosen for investigation are base shear, isolating displacement (base movement of structure corresponding to ground), and control force at base. Shear at the base directly correlates with seismic force transmission, and effective isolation depends on keeping sliding displacement within prescribed limits.

3.1. Performance Evaluation of the Proposed Controller under Harmonic Ground Acceleration

The success of the presented control method is assessed by applying harmonic ground acceleration $\ddot{x}_g(t) = 0.3g\sin(\omega t)$ to a controlled structure (FPS-isolated structure with PID controller) and comparing its response to that of an uncontrolled structure (FPS isolated structure without PID controller) across a range of excitation frequencies, ω. Figures 4a-4b compare sliding displacement and shear at the base in controlled and uncontrolled 2DOF isolated structures. The figures show that as expected, base shear and isolating displacement decrease with lower excitation frequencies, increasing to a peak value as excitation frequency approaches FPS isolator's frequency (at $\omega = \omega_r = 2.5$ rad/sec).

With further increase in excitation frequency, the responses of the structure decrease, indicating a resonance problem, which is the major drawback of the FPS isolated structure. However, it is clear from Figures 4a-4b that both displacement due to isolation and shear at base in the controlled structure do not vary much with excitation frequency and are almost similar at all the frequencies, indicating that the isolated structure response is more or less not dependent on the excitation frequency. This is a major advantage of controlling the isolated structure. Further, Figures 4a-4b reveal that peak shear at base and peak isolating displacement of uncontrolled structure are equal to 4306.5 kN and 2203.6 mm respectively. However, these responses reduce to 1600.8 kN and 701.1 mm respectively.

Above observations clearly demonstrate the effectiveness of proposed PID controller to decrease both the sliding displacement and base shear simultaneously. Moreover, the proposed controller shows almost similar responses at almost all the excitation frequencies without inducing any resonance problem.

Figure 4c illustrates the control force variation with frequency of excitation for the structure controlled. Figure shows an increase of control force from 369.6 kN at $\omega = 1$ rad/sec to 944.75 kN at $\omega = 2$ rad/sec. However, with further increase in excitation frequency, the control force reduces to 275 kN. This shows that the intelligent PID controller predicts a large control force to suppress huge shear at base and isolating displacement close to the frequency of resonance ($\omega = \omega_r$). Nevertheless, the controller adjusts control force to be lower at other frequencies, preventing increased base shear and ensuring a uniform response across frequencies.

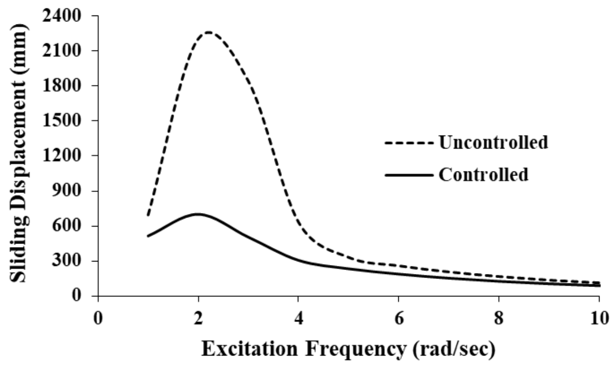

(a) Sliding displacement vs. excitation frequency

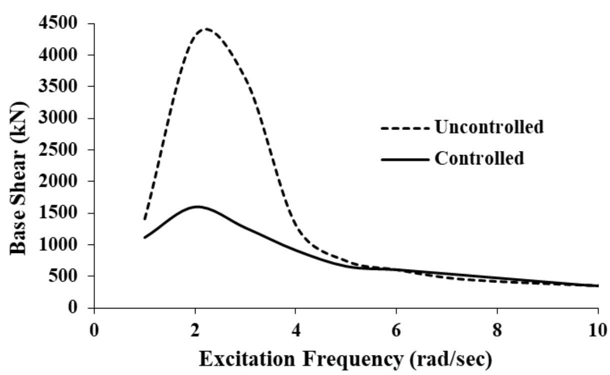

(b) Base shear vs. excitation frequency

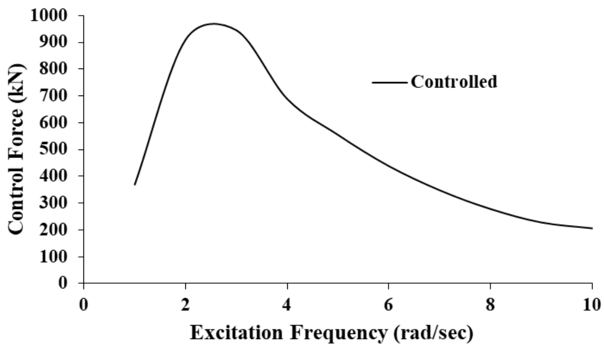

(c) Control force vs. excitation frequency

Figure 4 (a). Sliding displacement response of the structure for various excitation frequencies. (b) Base shear response of the structure for various excitation frequencies. (c) Variation of control force with excitation frequencies for 2DOF structure

3.2. Performance Evaluation of the Proposed Controller under Real Seismic Ground Motions

This section discusses, effectiveness of proposed PID controller is assessed under five real earthquake motions, namely, far-field (FF) 1940 El Centro earthquake (PGA 3.41m/sec^2), near-fault (NF) earthquakes that include 1979 Imperial Valley earthquake (PGA 4.28 m/sec^2), 1994 Northridge earthquake (PGA 8.27m/sec^2), 1999 Chi-Chi earthquake (PGA 4.97 m/sec^2) and 1995 Kobe earthquake (PGA 6.04 m/sec^2).

The base shear and isolating displacement time history responses in controlled and uncontrolled FPS isolated structures are shown in Figures 5-9 for five earthquakes, along with their respective peak values. Figures 5-9 demonstrate that a controlled structure exhibits lesser base shear and sliding displacement compared to an uncontrolled structure at all the time intervals during earthquake ground motions. This illustrates the usefulness of adopted PID controller to control responses of the FPS structure for various types of earthquakes having different magnitudes and characteristics. As shown in the figures for the El Centro earthquake (FF), the peak sliding displacement is reduced from 108.8 mm to 61.5 mm without much decline in base shear. Notably, the controller achieves substantial reductions in peak isolating displacement and peak shear at base, simultaneously for all earthquakes. The Chi-Chi earthquake, with the strongest near-fault characteristics, exhibits the largest reductions in peak sliding displacement (72.1%) and peak base shear (66.4%) compared to other near-fault earthquakes. For other types of NF earthquakes, the fall in base shear is in the range of 43.6 % to 46.1 % and the decline in sliding displacement is in the range of 61.1 % to 66.7 %. This clearly showcases the ability of the controller implemented to suppress large responses caused by long-period waves in the structure, which is the major characteristic of near-fault earthquakes. While for the far-field El Centro earthquake, the effect of PID controller is not as significant comparable to near- fault seismic excitations, but it still effectively reduces isolation displacement without amplifying shear at the base.

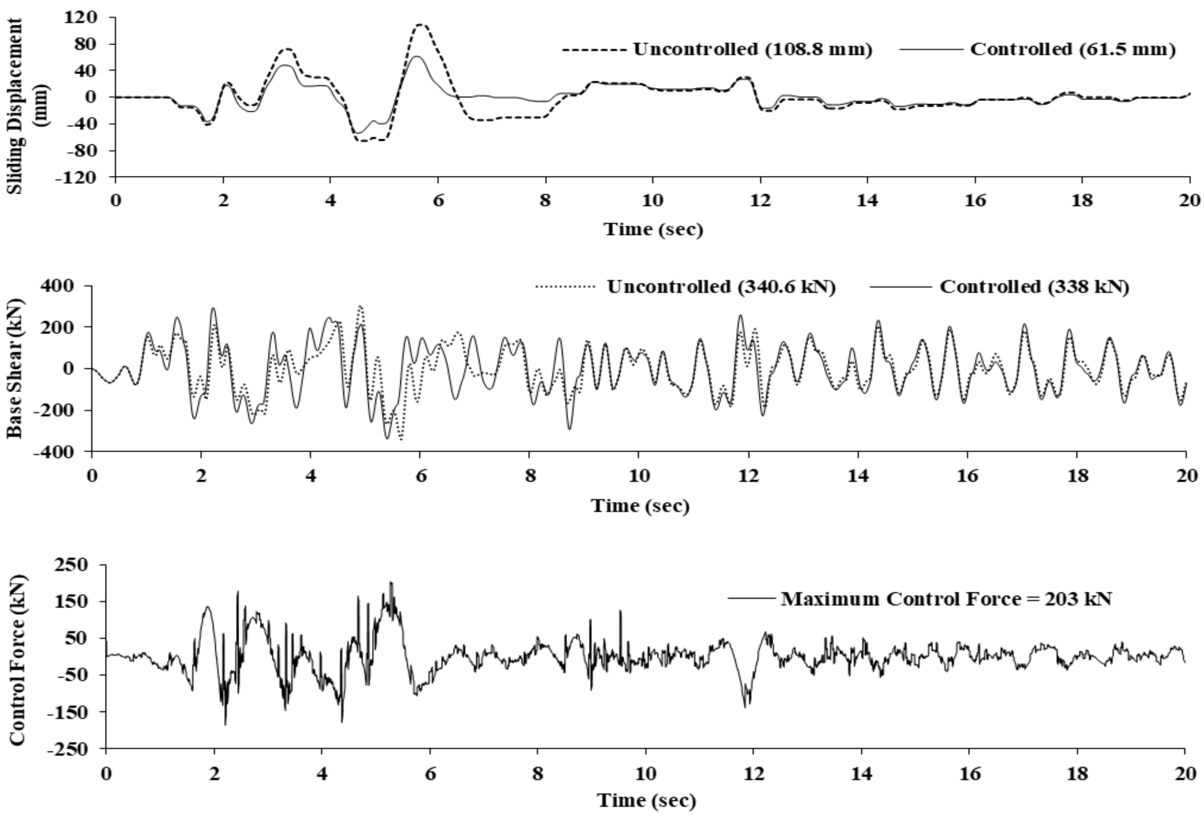

Figure 5. El Centro earthquake response of structures: controlled vs. uncontrolled

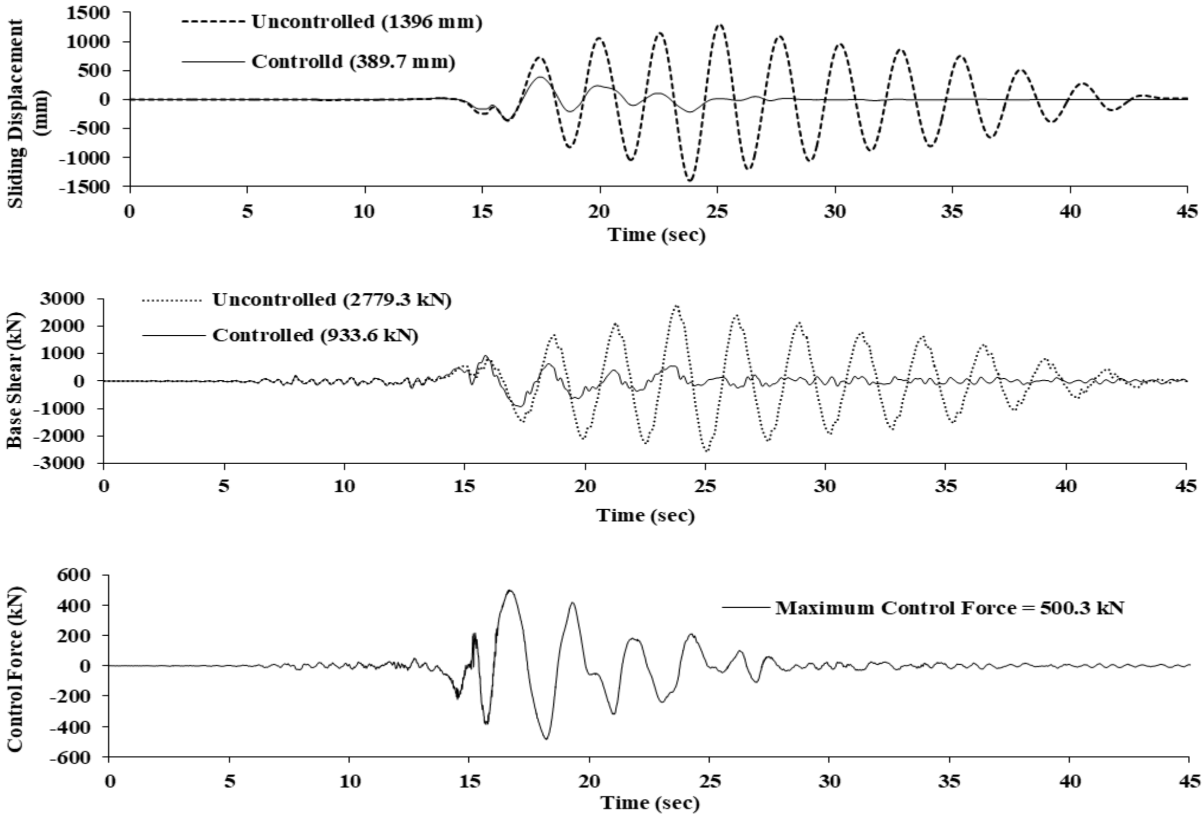

Figure 6. Chi-Chi earthquake response of structures: controlled vs. uncontrolled

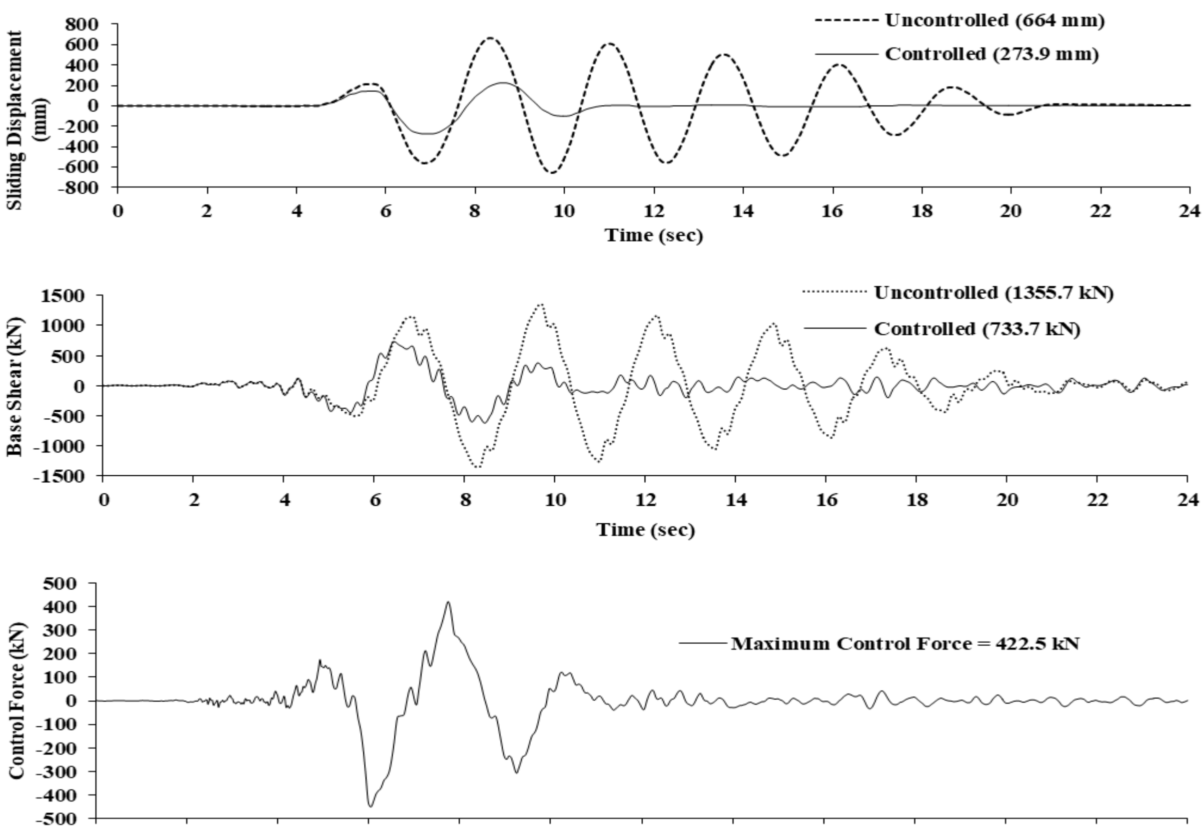

Figure 7. Imperial Valley earthquake response of structures: controlled vs. uncontrolled

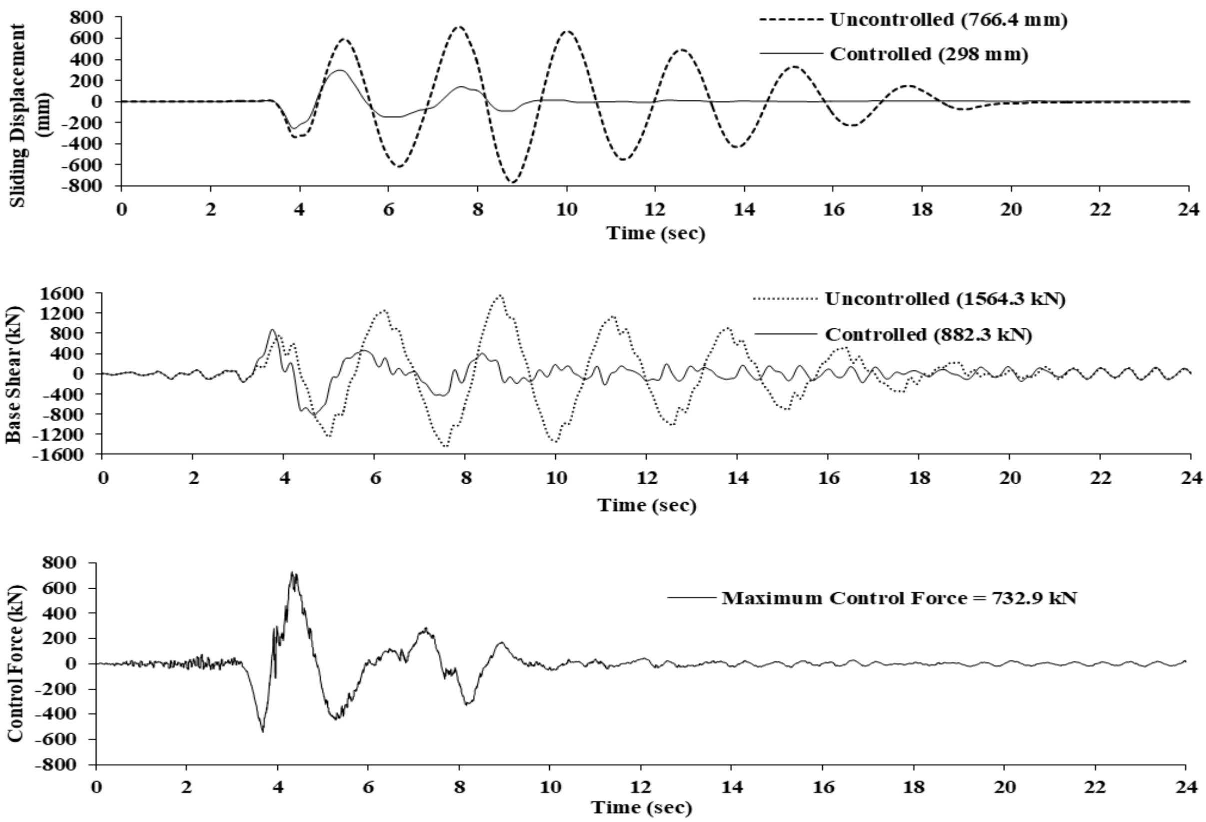

Figure 8. Northridge earthquake response of structures: controlled vs. uncontrolled

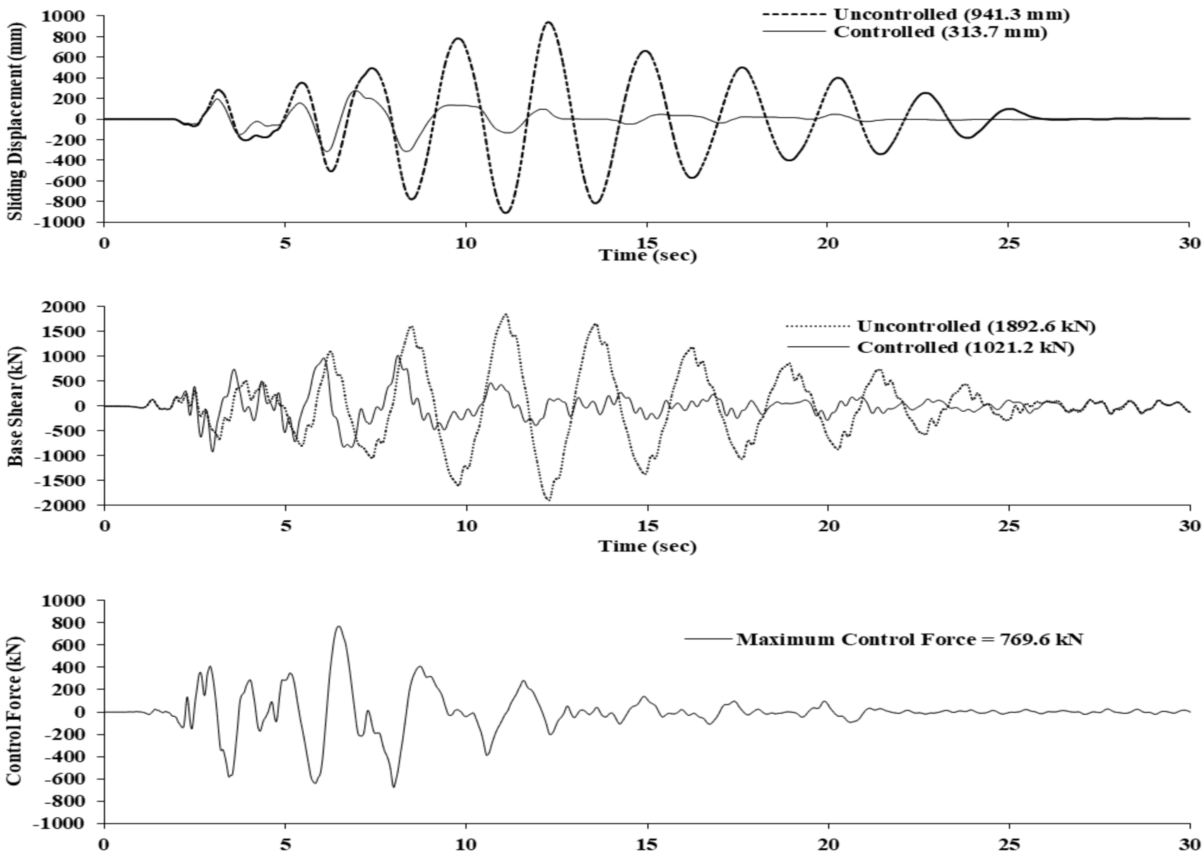

Figure 9. Kobe earthquake response of structures: controlled vs. uncontrolled

The control force variation over various intervals of time along with peak control forces in the PID-controlled isolated structure during earthquake ground motion is illustrated in Figures 5-9. These figures clearly show that, unlike passive dampers, control force generated by the implemented controller is not similar at all-time intervals. The intelligent controller predicts larger control force corresponding to larger shear at base in order to mitigate the larger shear at the base and larger sliding displacement, whereas, for other time intervals at lesser shear at base the proposed controller predicts lesser control force to prevent an increase in base shear due to excess control force.

Figures also show the peak control force predicted by the controller is also not similar for every earthquake ground motion. The peak control force projected using PID technique is smallest for El Centro earthquake and is equal to 203.4 kN, whereas it is maximum for Kobe earthquake and is equal to 769.6 kN.

It may be noted that one of the techniques proposed over time to control isolated structure response is the passive viscous fluid damper (VFD). The structural response achieved with VFD, however, depends on the damping coefficient of the VFD. Krishnamoorthy et al. [37] found that passive dampers exhibit a drop in sliding displacement with increasing value of damping coefficient, while initially shear at the base decreases, attains its minimum, and again rises with additional damping coefficient increments, suggesting an optimal damping coefficient for minimum base shear. However, as observed from equation 5, the forces applied by the isolator with damper are dependent on the isolation device properties (radius and coefficient of friction) and on the damping force (F_c) of VFD. The optimum damping coefficient of a passive damper intended for optimal response to one type of earthquake, may not be optimal for another type since F_c is not dependent on ground acceleration force $F(t)$. However, in a semi-active VFD, the coefficient of damping or the damping force is controllable for different earthquakes to obtain optimal response across all types of earthquakes. The optimum response for a structure isolated with the passive damper is obtained by varying the damping ratio from 0 to 1.8 in increments of 0.1 considering all earthquake types [37]. The optimum base shear responses obtained are equal 283.4 kN, 944.6 kN, 634.9 kN, 928.7 kN, and 892.3 kN respectively for El Centro, Chi-Chi, Imperial Valley, Northridge, and Kobe earthquakes. Due to the variation in the control force (F_c) for different earthquakes as predicted by PID controller, the optimum responses, as observed from Figures 5-9 are almost similar to the responses obtained by the proposed technique for a PID controlled semi-active device. Unlike passive VFD damper, where damping force (F_c) does not vary across earthquake types, a semi-active VFD controlled using a PID controller, varies the damping force (F_c) based on the earthquake type to produce optimal responses for various seismic events. This is the reason for the reduction in structural response in the case of a semi-active device isolated structure and also for achieving a similar response to optimum passive damper.

3.3. Peak Responses versus PGA

This section aims to investigate the usefulness of PID controller technique in governing the performance of 2DOF isolated structure for the five earthquakes at various PGA levels ranging from 0.1g to 1g. By this, the peak ground accelerations for all five earthquakes are made equal, whereas the frequency content of different earthquakes is different. This study also assesses the efficiency of PID controller in controlling the isolated structure subjected to earthquakes with different frequency content and similar PGA levels. The base shear response and displacement due to sliding in controlled and uncontrolled structures for various levels of PGA are compared in Figures 10-14. Effectiveness to control these responses for the earthquakes of different frequency content at PGA levels ranging from 0.1 g to 1g is clearly observed from these figures. The controller is less effective at lower PGA and its effectiveness increases as the PGA increases. The peak shear response at the base and displacement due to sliding of the uncontrolled structure amplify significantly as PGA increases for near-fault earthquakes, whereas, the control method adopted is efficient in controlling these responses at all values of PGA for both NF and FF earthquake excitations based on different frequency content.

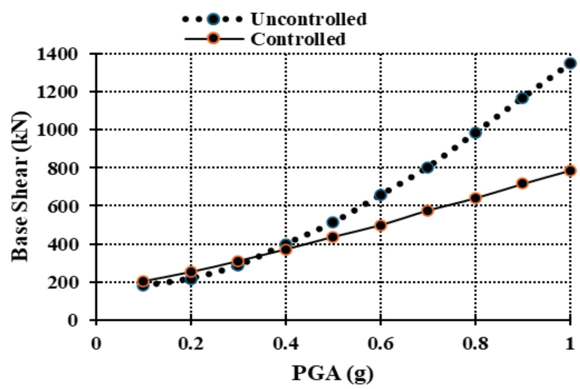

Figure 10. PGA v/s response for El Centro earthquake

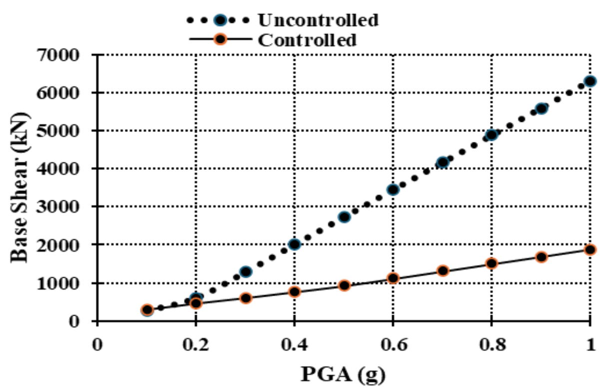

Figure 11. PGA v/s response for Chi-Chi earthquake

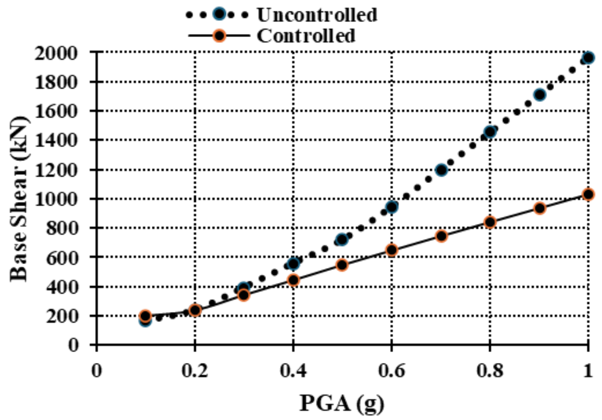

Figure 12. PGA v/s response for Northridge earthquake

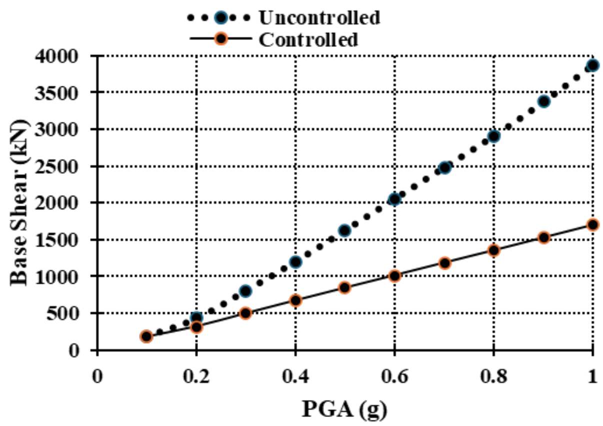

Figure 13. PGA v/s response for Imperial Valley earthquake

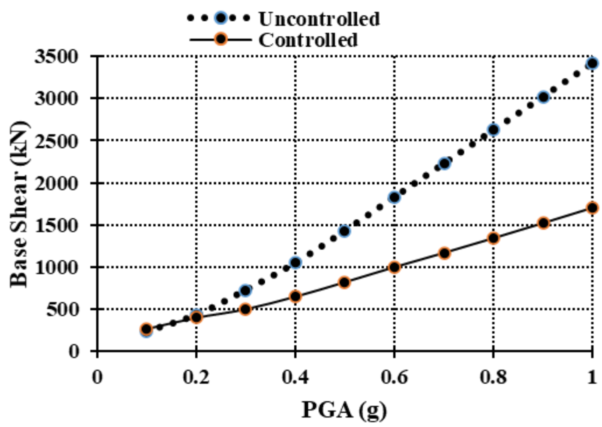

Figure 14. PGA v/s response for Kobe earthquake

4. Summary and Conclusions

Structures isolated with FPS can be susceptible to resonance issues when subjected to near-fault earthquakes. Passive devices optimized for one type of earthquake may not perform well under different seismic events. This study utilises PID control technique to address these limitations. The effectiveness of the PID control method is investigated for a 2DOF isolated structure, demonstrating its potential to enhance the response of the structure during earthquakes. The assessment concludes that the PID controller offers a simple solution, as its parameters can be easily determined, making it a practical and efficient control strategy. The presented PID control method is efficient in reducing base shear and sliding displacement during near-fault earthquakes, without increasing the responses during far-field earthquakes. Thus, the controller is equally effective for both far-field and near-fault seismic activities. Further, the responses simulated by the suggested control technique are more or less similar at all excitation frequencies, nullifying the resonance problem of the structure having FPS isolation.

Notably, the current investigation focuses on the efficiency of semi-active devices confined to the isolation system, although future studies considering their impact on the performance of the superstructures are to be additionally accounted for. In addition, the applicability of the proposed technique is studied analytically for a 2DOF model as available in the literature. To apply the technique to practical engineering applications, the impact of the proposed technique needs to be studied for real MDOF structures using analytical and experimental models.

REFERENCES

[1] Chae Y. and Ricles J. M., "Seismic performance enhancement of base-isolation using semi-active damping devices," in Proceedings of 15th World Conferences on Earthquake Engineering, Lisbon, Portugal, September 2012. https://www.iitk.ac.in/nicee/wcee/article/WCEE2012_5568.pdf

[2] Zayas V. A., Low S. S., and Mahin S. A., "A simple pendulum technique for achieving seismic isolation," Earthquake Spectra, vol. 6, no. 2, pp. 317-333, 1990. DOI: 10.1193/1.1585573.

[3] Thomas T., Mathai A., "Study of base isolation using friction pendulum bearing system," IOSR Journal of Mechanical and Civil Engineering, pp. 19-23, 2016. https://www.iosrjournals.org/iosr-jmce/papers/ICETEM/Vol.%201%20Issue%202/17-19-23.pdf.

[4] Pranesh M., Sinha. R., "VFPI: an isolation device for aseismic design," Earthquake Engineering & Structural Dynamics, vol. 29, no. 5, pp. 603-627, 2000. DOI: 10.1002/(SICI)1096-9845(200005)29:5<603::AID-EQE927>3.0.CO;2-W.

[5] Lu L. Y., Wang J., Hsu C. C., "Sliding isolation using variable frequency bearings for near-fault ground motions," in 4th International Conference on Earthquake Engineering, Taipei, Taiwan, no. 164, 2006, pp. 1-10. https://shorturl.at/tGSNC.

[6] Xia Y., Ghasempoor A., "Active vibration suppression using neural networks," in Proceedings of the World Congress on Engineering, vol. 2, pp. 1-6, 2009. https://shorturl.at/gtNm3.

[7] Nishitani A., Inoue Y., "Overview of the application of active/semiactive control to building structures in Japan," Earthquake Engineering & Structural Dynamics, vol. 11, no. 30, pp. 1565-1574, 2001. DOI: 10.1002/eqe.81.

[8] Soong, T. T., Reinhorn A. M., Wang Y. P., Lin R. C., "Full-scale implementation of active control. I: Design and simulation," Journal of Structural Engineering, vol. 117, no. 11, pp. 3516-3536, 1991. DOI: 10.1061/(ASCE)0733-9445(1991)117:11(3516).

[9] Soldatos, A. G., Arvanitis K. G., Zacharenakis E. C., "Active control schemes for aseismic base-isolated structures," Archive of Applied Mechanics, vol. 72, pp. 147-159, 2002. DOI: 10.1007/s00419-001-0192-7.

[10] Al-Dawod M., Samali B., Kwok K., Naghdy F., "Fuzzy controller for seismically excited nonlinear buildings," Journal of Engineering Mechanics, vol. 130, no. 4, pp. 407-415, 2004. DOI: 10.1061/(ASCE)0733-9399(2004)130:4(407).

[11] Ahlawat, A. S., and Ramaswamy A., "Multiobjective optimal fuzzy logic controller driven active and hybrid control systems for seismically excited nonlinear buildings," Journal of Engineering Mechanics, vol. 130, no. 4, pp. 416-423, 2004. DOI: 10.1061/(ASCE)0733-9399(2004)130:4(416).

[12] Guclu R., "Sliding mode and PID control of a structural system against earthquake," Mathematical and Computer Modelling, vol. 44, no. 1-2, pp. 210-217, 2006. DOI: 10.1016/j.mcm.2006.01.014.

[13] Korkmaz S., "A review of active structural control: challenges for engineering informatics," Computers & Structures, vol. 89, no. 23-24, pp. 2113-2132, 2011. DOI: 10.1016/j.compstruc.2011.07.010.

[14] Fu, S. T., Johnson E. A., "Active control for a distributed mass damper system," Journal of Engineering Mechanics, vol. 140, no. 2, pp. 426-429, 2014. DOI: 10.1061/(ASCE)EM.1943-7889.0000650.

[15] Shariatmadar H., Razavi H. M., "Seismic control response of structures using an ATMD with fuzzy logic controller and PSO method," Structural Engineering Mechanics, vol. 51, no. 4, pp. 547-564, 2014. DOI: 10.12989/sem.2014.51.4.547.

[16] Pozo F., Pujol G., Acho L., "Vibration control of hysteretic base-isolated structures: an LMI approach," Smart Structures and Systems, vol. 17, no. 2, pp. 195-208, 2016. DOI: 10.12989/sss.2016.17.2.195.

[17] Moghaddasie B., Jalaeefar A., "Optimization of LQR method for the active control of seismically excited structures," Smart Structures and Systems, vol. 23, no. 3, pp. 243-261, 2019. DOI: 10.12989/sss.2019.23.3.243.

[18] Spencer Jr. B. F., Soong T. T., "New applications and development of active, semi-active and hybrid control techniques for seismic and non-seismic vibration in the USA," in Proceedings of international post-SMiRT conference seminar on seismic isolation, passive energy dissipation and active control of vibration of structures, Cheju, Korea, August 1999, pp. 23-25. https://sstl.cee.illinois.edu/papers/smirt99.pdf.

[19] Kumar G., Kumar R., Kumar A., "A review of the controllers for structural control," Archives of Computational Methods in Engineering, vol. 30, no. 6, pp. 3977-4000, 2023. DOI: 10.1007/s11831-023-09931-y.

[20] Hrovat D., Barak P., & Rabins M., "Semi-Active Versus Passive Or Active Tuned Mass Dampers For Structural Control," Journal of Engineering Mechanics, vol. 109, no. 3, pp. 691-705, 1983. DOI: 10.1061/(ASCE)0733-9399(1983)109:3(691).

[21] Dyke S. J., Spencer Jr. B. F., Sain M. K., Carlson J. D., "Modeling and control of magnetorheological dampers for seismic response reduction," Smart Materials and Structures, vol. 5, no. 5, pp. 565-575, 1996. DOI: 10.1088/0964-1726/5/5/006.

[22] Spencer Jr. B. F., Sain M. K., "Controlling buildings: a new frontier in feedback," IEEE Control Systems Magazine, vol. 17, no. 6, pp. 19-35, 1997. DOI: 10.1109/37.642972.

[23] Symans, Michael D., and Michael C. Constantinou, "Semi-active control systems for seismic protection of structures: a state-of-the-art review," Engineering structures, vol. 21, no. 6, pp. 469-487, 1999. DOI: 10.1016/S0141-0296(97)00225-3.

[24] Wongprasert N., Symans M. D., "Numerical evaluation of adaptive base-isolated structures subjected to earthquake ground motions," Journal of Engineering Mechanics, vol. 131, no. 2, pp. 109-119, 2005. DOI: 10.1061/(ASCE)0733-9399(2005)131:2(109).

[25] Sahasrabudhe, S. S., Nagarajaiah, S., "Semi-active control of sliding isolated bridges using MR dampers: an experimental and numerical study," Earthquake Engineering & Structural Dynamics, vol. 34, no. 8, pp. 965-983, 2005. DOI: 10.1002/eqe.464.

[26] Jung H. J., Choi K. M., Spencer Jr. B. F., Lee, I. W., "Application of some semi-active control algorithms to a smart base-isolated building employing MR dampers," Structural Control and Health Monitoring: The Official Journal of the International Association for Structural Control and Monitoring and of the European Association for the Control of Structures, vol. 13, no. 2-3, pp. 693-704, 2006. DOI: 10.1002/stc.106.

[27] Qi X. J., Li X. J., Tang H., "Study on semi-active control of seismic bend torsion coupling for curved bridge," Journal of Highway and Transportation Research and Development (English Edition), vol. 2, no. 1, pp. 48-52, 2007. DOI: 10.1061/JHTRCQ.0000167.

[28] Lu L. Y., Lin G. L., Kuo T. C., "Stiffness controllable isolation system for near-fault seismic isolation," Engineering Structures, vol. 30, no. 3, pp. 747-765, 2008. DOI: 10.1016/j.engstruct.2007.05.022.

[29] Ying Z. G., Ni Y. Q., Ko J. M., "A semi-active stochastic optimal control strategy for nonlinear structural systems with MR dampers," Smart Structures and Systems, vol. 5, no. 1, pp. 69-79, 2009. DOI: 10.12989/sss.2009.5.1.069.

[30] Karamodin K. A., Kazemi H. H., "Semi-active control of structures using neuro-predictive algorithm for MR dampers," Structural Control and Health Monitoring: The Official Journal of the International Association for Structural Control and Monitoring and of the European Association for the Control of Structures, vol. 17, no. 3, pp. 237-253, 2010. DOI: 10.1002/stc.278.

[31] Laflamme S., Slotine J. J. E., Connor J. J., "Wavelet

network for semi-active control. Journal of Engineering Mechanics, vol. 137, no. 7, pp. 462-474, 2011. DOI: 10.1061/(ASCE)EM.1943-7889.0000248.

[32] Woo S. S., Lee S. H., Chung L., "Seismic response control of elastic and inelastic structures by using passive and semi-active tuned mass dampers," Smart Structures and Systems, vol. 8, no. 3, pp. 239-252, 2011. DOI: 10.12989/sss.2011.8.3.239.

[33] Zhou Z., Meng S. P., Wu J., Zhao Y., "Semi-active control on long-span reticulated steel structures using MR dampers under multi-dimensional earthquake excitations," Smart Structures and Systems, vol. 10, no. 6, pp. 557-572, 2012. DOI: 10.12989/sss.2012.10.6.557.

[34] Chang C. M., Wang Z., Spencer B. F., Chen, Z., "Semi-active damped outriggers for seismic protection of high-rise buildings," Smart Structures and Systems, vol. 11, no. 5, pp. 435-451, 2013. DOI: 10.12989/sss.2013.11.5.435.

[35] Ghaffarzadeh H., "Semi-active structural fuzzy control with MR dampers subjected to near-fault ground motions having forward directivity and fling step," Smart Structures and Systems, An International Journal, vol. 12, no. 6, pp. 595-617, 2013. DOI: 10.12989/sss.2016.18.6.1111.

[36] Esteki K., Bagchi A., & Sedaghati R., "Semi-active control of seismic response of a building using MR fluid-based tuned mass damper," Smart Structures and Systems, vol. 16, no. 5, pp. 807-833, 2015. DOI: 10.12989/sss.2015.16.5.807.

[37] Krishnamoorthy A., Bhat S., Bhasari D., "Radial basis function neural network algorithm for semi-active control of base-isolated structures," Structural Control and Health Monitoring, vol. 24, no. 10, pp. e1984, 2017. DOI: 10.1002/stc.1984.

[38] Braz-Cesar M. T., Barros R. C., "Semi-active fuzzy based control system for vibration reduction of a SDOF structure under seismic excitation," Smart structures and systems, vol. 21, no. 4, pp. 389-395, 2018. DOI: 10.12989/sss.2018.21.4.389.

[39] Peng P., Dongbin Z., Yi Z., Yachun T., Xin N., "Development of a tunable friction pendulum system for semi-active control of building structures under earthquake ground motions," Earthquake Engineering & Structural Dynamics, vol. 47, no. 8, pp. 1706-1721, 2018. DOI: 10.1002/eqe.3036.

[40] Zhang D., Pan P., Zeng Y., Guo Y., "A novel robust optimum control algorithm and its application to semi-active controlled base-isolated structures," Bulletin of Earthquake Engineering, vol. 18, pp. 2431-2460, 2020. DOI: 10.1007/s10518-019-00761-7.

[41] Tai W. C., Ikenaga M., "A semi-active control system in coupled buildings with base-isolation and magnetorheological dampers using an adaptive neuro-fuzzy inference system," Frontiers in Built Environment, vol. 8, pp. 1-15, 2022. DOI: 10.3389/fbuil.2022.1057962.

[42] Etedali S., Zamani A. A., "Semi-active control of nonlinear smart base-isolated structures using MR damper: sensitivity and reliability analyses," Smart Materials and Structures, vol. 31, no. 6, pp. 065021, 2022. DOI: 10.1088/1361-665X/ac6d32.

[43] Jangid R. S., "Seismic performance assessment of clutching inerter damper for isolated bridges," Practice Periodical on Structural Design and Construction, vol. 27, no. 2, pp. 04021078, 2022. DOI: 10.1061/(ASCE)SC.1943-5576.0000661.

[44] Zheng S., Shen Q., Guan C., Cheng H., Zhuang H., Zhou M., "Semi-active control of seismic response on prestressed concrete continuous girder bridges with corrugated steel webs," Applied Science, vol. 12, no. 24, pp. 12881, 2022. DOI: 10.3390/app122412881.

[45] Thenozhi S., Yu W., "Stability analysis of active vibration control of building structures using PD/PID control," Engineering Structures, vol. 81, pp. 208-218, 2014. DOI: 10.1016/j.engstruct.2014.09.042.

[46] Åström K. J., Hägglund T., "The future of PID control," Control Engineering Practice, vol. 9, no. 11, pp. 1163-1175, 2001. DOI: 10.1016/S0967-0661(01)00062-4.

[47] Jung W. J., Jeong W. B., Hong S. R., Choi S. B., "Vibration control of a flexible beam structure using squeeze-mode ER mount," Journal of Sound and Vibration, vol. 273, no. 1-2, pp. 185-199, 2004. DOI: 10.1016/S0022-460X(03)00478-4.

[48] Fung R. F., Liu Y. T., Wang C. C., "Dynamic model of an electromagnetic actuator for vibration control of a cantilever beam with a tip mass," Journal of Sound and Vibration, vol. 288, no. 4-5, pp. 957-980, 2005. DOI: 10.1016/j.jsv.2005.01.046.

[49] Guclu R., Yazici H., "Fuzzy logic control of a non-linear structural system against earthquake induced vibration," Journal of Vibration and Control, vol. 13, no. 11, pp. 1535-1551, 2007. DOI: 10.1177/1077546307077663.

[50] Guclu R., Yazici H., "Seismic-vibration mitigation of a nonlinear structural system with an ATMD through a fuzzy PID controller," Nonlinear Dynamics, vol. 58, pp. 553-564, 2009. DOI: 10.1007/s11071-009-9500-5.

[51] Etedali S., Sohrabi M. R., Tavakoli S., "Optimal PD/PID control of smart base isolated buildings equipped with piezoelectric friction dampers," Earthquake Engineering and Engineering Vibration, vol. 12, no. 1, pp. 39-54, 2013. DOI: 10.1007/s11803-013-0150-8.

[52] Nigdeli S. M., & Boduroğlu M. H., "Active tendon control of torsionally irregular structures under near-fault ground motion excitation," Computer-Aided Civil and Infrastructure Engineering, vol. 28, no. 9, pp. 718-736, 2013. DOI: 10.1111/mice.12046.

[53] Etedali S., & Tavakoli S., "PD/PID controller design for seismic control of high-rise buildings using multi-objective optimization: a comparative study with LQR controller," Journal of Earthquake and Tsunami, vol. 11, no. 03, pp. 1750009, 2017. DOI: 10.1142/S1793431117500099.

[54] Şen A., M., Tinkir M., & Kalyoncu M., "Optimisation of a PID controller for a two-floor structure under earthquake excitation based on the bees algorithm," Journal of Low Frequency Noise, Vibration and Active Control, vol. 37, no.1, pp. 107-127, 2018. DOI: 10.1177/1461348418757906.

[55] Heidari A. H., Etedali S., Javaheri-Tafti M. R., "A hybrid LQR-PID control design for seismic control of buildings equipped with ATMD," Frontiers of Structural and Civil

Engineering, vol. 12, no. 1, pp. 44-57, 2018. DOI: 10.1007/s11709-016-0382-6.

[56] Wang X., & Qu Z., "Uncertainty in the seismic performance of semi-active base isolation systems," Earthquake Research Advances, vol. 3, no. 2, pp. 100173, 2023. DOI: 10.1016/j.eqrea.2022.100173.

[57] Bhowmik K., Debnath N., "Semi-active vibration control of soft-storey building with magnetorheological damper under seismic excitation," Journal of Vibration Engineering & Technologies, vol. 12, no. 4, pp. 6943-6961, 2024. DOI: 10.1007/s42417-024-01292-5.

[58] Sharma S. K., Sharma R. C., Lee, J., "Modelling and simulation of MR damper characterization and uncertainty assessment in marine engine vibration isolation with FLPID control," International Journal of Modelling and Simulation, pp. 1-11, 2024. DOI: 10.1080/02286203.2024.2327465.

[59] Vides S., Castillo B., Artunduaga A., Marulanda J., Thomson, P., "Assessment of a base-isolated structure with semi-active low-cost viscous fluid dampers through real-time hybrid simulations," Innovative Infrastructure Solutions, vol. 10, pp. 123, 2025. DOI: 10.1007/s41062-025-01901-6.

[60] Yang Y. B., Lee T. Y., Tsai I.C., "Response of multi-degree-of-freedom structures with sliding supports," Earthquake Engineering & Structural Dynamics, vol. 19, no. 5, pp. 739-752, 1990. DOI: 10. 1002/eqe.4290190509.

[61] Wang Q. G., Lee T. H., Fung H. W., Bi Q., Zhang Y., "PID tuning for improved performance," IEEE Transactions on Control Systems Technology, vol. 7, no. 4, pp. 457-465, 1999. DOI: 10.1016/j.eqrea.2022.100173.

[62] Thirunavukkarasu I., George V. I., Iyer S. N., Kumar G. S., Al-Abrii Y., "Admissible set of robust PID controller values using Hurwitz Criterion for a Pure Integrating Process with dead time," International Journal of Applied Engineering Research, vol. 3, no. 11, pp. 1507-1522, 2008. https://shorturl.at/yep8j.

[63] Banerjee A., Bhattacharjee S., Neogi B., "Tuning of PID Controller Using Bode Plot Technique towards the Dynamics of Human Cardiac Muscle Considering Dead Time," International Journal of Advanced Scientific Research and Management, vol. 4, no. 6, pp. 110-115, 2019. https://shorturl.at/SwajJ.